

Permanent magnetic microtraps for ultracold atoms

Amir Mohammadi, Saeed Ghanbari and Aref Pariz

Department of Physics, Faculty of Science, University of Zanjan, 45371-38791
Zanjan, Iran

E-mail: amir.mohammadi@uni-ulm.de, sghanbari@znu.ac.ir,
aref_pariz@znu.ac.ir

Abstract. We propose and numerically study two permanent magnetic microstructures for creating Ioffe-Pritchard microtraps. A bias magnetic field is used to vary the depth, trap frequencies and the minimum of each microtrap. After the Bose-Einstein condensation achievement, the bias magnetic field can be slowly removed to increase the trap barrier heights for more efficiently holding the Bose-Einstein condensates. Even without the external magnetic field, it is possible to hold ultracold atoms in the microtraps. These microtraps may also be useful for single atom experiments for quantum information processing due to their very high confinement.

PACS numbers: 67.85.Hj, 37.10.Gh, 37.10.De, 85.85.+j

1. Introduction

After the experimental realization of the Bose-Einstein condensation (BEC) in 1995 [1, 2], the study of ultracold Bose and Fermi gases has become one of the most active fields of research in atomic physics [3, 4, 5, 6, 7]. Neutral atoms can be trapped in the non-zero minimum of a magnetic field gradient. Magnetic microtraps can produce this spatial gradient to confine and guide neutral atoms in ultracold regimes and Bose-Einstein condensates [8, 9, 10]. Current-carrying wires are common tools to create magnetic microtraps [11, 12]. Large number of experiments have been done by using wire traps, ranged from single microtrap to arrays of microtraps to manipulate ultracold atoms and to realize the BEC [10, 13, 14, 15, 16, 17, 18, 19]. Beside wire traps, technological developments have provided us with high quality magnetic microstructures based on permanent magnetization as an alternative approach for creating lattices of microtraps for ultracold atoms [20, 21, 22, 23, 24, 25, 27, 28]. While wire-based traps involve high current densities, leading to trap loss and heating of atoms near surfaces, permanent magnetic microtraps can produce highly stable potential wells with low noise. Atom chips using permanent magnetic slabs are also preferred over wire-based magnetic traps for their better confinement features due to their high curvatures and for the freedom to vary the layout, design and magnitudes of the magnetic potentials. Like wire traps, permanent magnetic microtraps offer arrays of periodic microtraps [22, 24, 25, 26] and single microtrap [27]. Many experimental works in cold

atom physics with permanent magnetic traps have been reported and BEC has been demonstrated in various setups such as F-shaped permanent magnetic atom chip and 2D permanent magnetic lattices [18, 27, 29, 30, 31, 32, 33, 34]. Generally, atom chips are microscopic integrated matter-wave devices which can produce flexible potentials in space [22, 32, 35, 36, 37, 38]. They are used for investigation of the physics of correlated many-body quantum systems [39], matter-wave interferometry [19, 40, 41, 42] and phase transitions [43, 44]. Moreover, atom chips are suitable for the implementation of scalable quantum information processing [45, 46, 47]. Recently, multi-particle entanglement on an atom chip was experimentally realized, which is a useful resource for quantum metrology [48].

In this paper, we propose two simple Ioffe-Pritchard permanent magnetic atom chips for holding ultracold atoms and Bose-Einstein condensates. The microtraps are self-biasing and external bias fields can be used to change the magnetic field potential barrier heights for loading and manipulating ultracold atoms. Clouds of atoms can be moved adiabatically from a quadruple magnetic trap and loaded into the microtraps by varying external magnetic fields. This particular loading trajectory helps to avoid any secondary minimum (e.g., see [27]) as much as possible. The reverse process can be done to release cloud of atoms from trap. The main motivation of this work is introducing simple magnetic microtraps to hold atoms in ultracold regimes without bias field and offering a simple tool for changing the height of potential barriers in the microtrap. Similar to other experiments, using Radio Frequency (RF) waves, clouds of ultracold atoms are forced to evaporate during loading process or after that [3, 19, 27]. However, there is also another way for ejecting energetic atoms from trap by tuning external magnetic field. This method is not recommended in our case due to low gain of evaporative cooling which is not in all three directions of the trap, but can be used beside other methods for effective cooling. We have performed numerical calculations for two relatively low and high magnetization values 800 and 3800 G. The results are presented for structures in different scales to give some perspective to experimentalists. Our calculations for ^{87}Rb atoms predict relatively high BEC transition temperatures (i.e. several μK) which could be interesting. The method has been proposed in a novel simple three-wire-based magnetic microtrap[35], where barrier heights of the trapping potential are lowered so that the atoms with higher energies are removed from the trap [3, 19].

2. U- and H-like-shaped fully permanent atom chips

figure 1 shows a U-shaped microstructure consisting of three permanent magnetic slabs. This structure can produce Ioffe-Pritchard microtraps. The two parallel (red) slabs have opposite magnetization along y direction while the middle (blue) one has same magnetization in the z direction. Magnetic field due to the parallel slabs is cancelled near the center of the trap. By adding the third slab with magnetization in the z direction, minimum of the magnetic field is increased to $B_{min} \neq 0$. Middle slab has a

thickness t_1 , the parallel ones have same thickness t_2 and all slabs have same length h and width a . Separation between the parallel slabs is d . This structure can be made by depositing every single magnetic slab on a larger nonmagnetic material (gray objects) on a desired scale, as we have shown in figure 1 and figure 3. In this paper, a perpendicular magnetization with two values $4\pi M \sim 800$ G and $4\pi M \sim 3800$ G has been assumed for all magnetic slabs. Materials such as Alnico alloys [50] (e.g., Alnico-5) and $Tb_6Gd_{10}Fe_{80}Co_4$ [22] with high Curie temperatures can be used for the magnetization values 800 and 3800 G, respectively. One can deposit the magnetic material in a strong magnetic field, below Curie temperature, to orient the magnetization in the desired direction and finally put all parts together to form the magnetic structures [51, 52]. The interaction potential energy between the atoms and the magnetic field is given by $U = \mu_B g_F m_F B$ where μ_B , g_F , m_F and B are the Bohr magneton, Landé factor, magnetic quantum number and magnetic field modulus, respectively. We consider ^{87}Rb atoms when the cloud is compressed (CMOT) and optically pumped to the quantum state $F = 2$ and $m_F = 2$ with the Landé factor 0.5 [3]. To do the numerical calculations, we have written a Mathematica code and have used the software package Radia [53] interfaced to Mathematica. The trap frequencies are determined for ^{87}Rb atoms using the relations $\omega_i = \gamma \sqrt{\partial^2 B / \partial x_i^2}$ at the minimum of the potential where $x_1 = x$, $x_2 = y$, $x_3 = z$, $\omega_1 = \omega_x$, $\omega_2 = \omega_y$, $\omega_3 = \omega_z$ and $\gamma = \sqrt{\mu_B g_F m_F / m}$. Here, m is the ^{87}Rb atom mass. To investigate how an external magnetic field can change the trap frequencies and also depth of the trap, an external magnetic field $\mathbf{B}_1 = B_{1z} \hat{z}$ is applied. We start from a relatively small trap structure (Scale A_U) with $h = 50 \mu\text{m}$, $a = 5 \mu\text{m}$, $d = 44 \mu\text{m}$, $t_1 = 2 \mu\text{m}$, $t_2 = 3 \mu\text{m}$ and low magnetization $4\pi M \sim 800$ G. According to figure 2, we have an Ioffe-Pritchard microtrap for this configuration and an external magnetic field in the z direction can change the depth of the microtrap and frequencies in the x and y directions but leaves its position and z unchanged. Moreover, the height of the potential barrier in each direction depends on the bias magnetic field. figure 2 also shows that the U-shaped permanent magnetic atom chip can produce a single magnetic microtrap either with a bias field or without it which may have applications in quantum information processing and data storage. For understanding the behaviour of the trap on different scales and magnetization values,

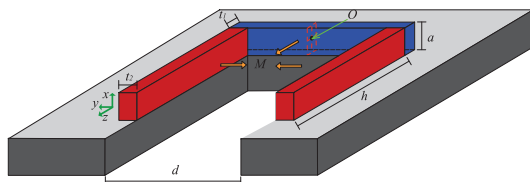


Figure 1. (color online). Schematic of a U-shaped microtrap. Thicknesses of the middle slab (blue) and the parallel ones (red slabs) are t_1 and t_2 , respectively. Separation between the parallel slabs is d . Magnetization is perpendicular to the biggest area of the magnets (orange arrows) and has same value for all slabs. Length and width of all slabs are h and a , respectively.

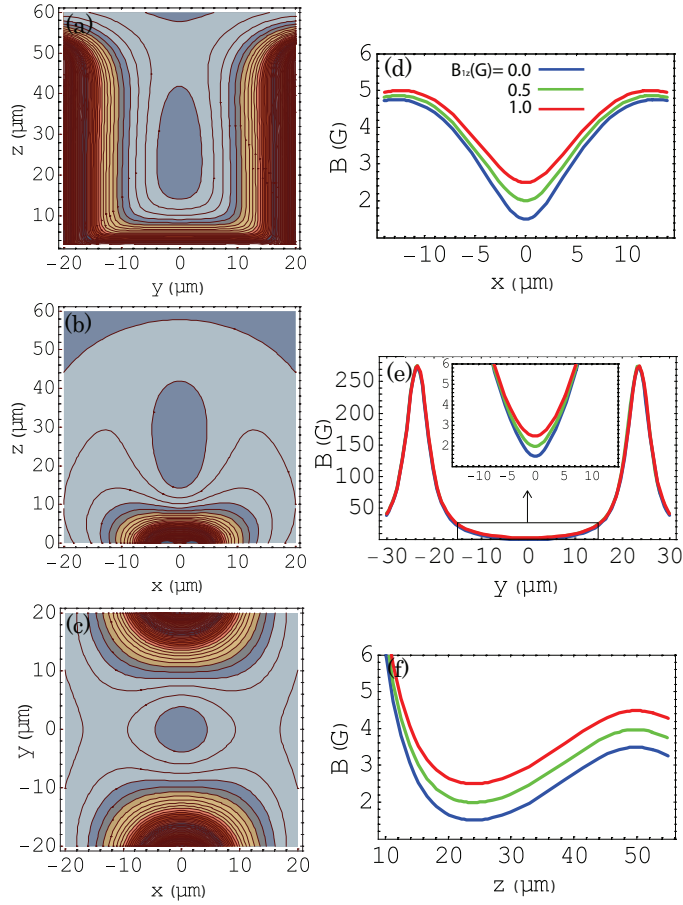


Figure 2. (color online). (a), (b) and (c) Contour plots of B , for the U-shaped microtrap described in figure 1, at $x = x_{min}, y = y_{min}$ and $z = z_{min}$ planes, respectively, when the external bias field is zero. Center of the microtrap is at $x_{min} = y_{min} = 0$ and $z_{min} = 24\mu\text{m}$. (d), (e) and (f) Plots of magnetic field along x , y and z directions, respectively, for $B_{1z} = 0, 0.5$ and 1.0 G. Plots show variation of B near the center of the microtrap. B_{min} has a the nonzero value of 1.5 G even when the bias field is zero. Parameters used for these plots are $h = 50\mu\text{m}$, $a = 5\mu\text{m}$, $d = 44\mu\text{m}$, $t_1 = 2\mu\text{m}$ and $t_2 = 3\mu\text{m}$ and $4\pi M \sim 800$ G.

we repeat our calculations for relatively high magnetization $4\pi M \sim 3800$ G on different scales. For the bias magnetic field $B_{1z} = 0$, the trap frequencies $\omega_x/2\pi$, $\omega_y/2\pi$ and $\omega_z/2\pi$ for both values of magnetization are given in table 1. This table shows that for $B_{1z} \neq 0$ all the frequencies are less than the corresponding values for $B_{1z} = 0$. Moreover, according to the table 1, second derivatives of the magnetic field modulus i.e. curvatures of B along x and y directions, decrease during the increase of the bias field from $B_{1z} = 0$. Table 1 shows that for equal magnetization, trap frequencies in small traps are bigger. For all scales, trap minimum depends on the magnetization of the structures and only changes when external bias field in z direction is applied.

$\Delta U^x/k_B$, $\Delta U^y/k_B$ and $\Delta U^z/k_B$ for all different trap configurations with and without B_{1z} are compared in table 2 where $\Delta U^i = U_{max}^i - U_{min}^i$. Here, $i=1, 2$ and 3

Table 1. Numerical results for U-shaped fully permanent magnetic chip (figure 1). Results are obtained in different magnetization values for ^{87}Rb in $F=2$ and $m_F=2$ state. On scale A_U we have $h = 50\mu\text{m}$, $a = 5\mu\text{m}$, $d = 44\mu\text{m}$, $t_1 = 2\mu\text{m}$ and $t_2 = 3\mu\text{m}$, while scales B_U and C_U are two and four times larger than scale A_U , respectively.

Parameter	Scale A_U		Scale A_U		Scale B_U		Scale C_U	
	0	1	0	3	0	3	0	3
$B_{1z}(\text{G})$								
$4\pi M(\text{G})$	800		3800		3800		3800	
$\frac{\partial^2 B}{\partial x^2} (\frac{\text{G}}{\text{cm}^2})$	2.5×10^5	1.4×10^5	1.2×10^8	8.1×10^7	2.9×10^7	2.0×10^7	7.4×10^6	5.1×10^6
$\frac{\partial^2 B}{\partial y^2} (\frac{\text{G}}{\text{cm}^2})$	2.6×10^5	1.6×10^5	1.2×10^8	8.7×10^7	3.1×10^7	2.1×10^7	7.7×10^6	5.4×10^6
$\frac{\partial^2 B}{\partial z^2} (\frac{\text{G}}{\text{cm}^2})$	1.6×10^4		1.6×10^6		1.8×10^6		4.6×10^5	
$\omega_x/2\pi(\text{kHz})$	6.4	4.9	1.3	1.15	0.69	0.57	0.34	0.28
$\omega_y/2\pi(\text{kHz})$	6.5	4.5	1.4	1.2	0.71	0.59	0.35	0.29
$\omega_z/2\pi(\text{kHz})$	1.6		0.24		0.17		0.08	
$z_{min} (\mu\text{m})$	24		24		72		96.2	
$B_{min} (\text{G})$	1.5	2.5	7.13	10.13	7.13	10.13	7.13	10.13

correspond to x , y and z , respectively. According to the table, this microtrap is highly asymmetric with respect to the barrier heights in the x and y directions. Energy level spacings $\hbar\omega_i/k_B$ along the x_i direction are other parameters which we have calculated for this microtraps in table 2. This table also clearly shows that traps with higher magnetization have larger potential barrier heights and can be used for better holding, cooling and trapping ultracold atoms. Actually, tables 1 and 2 indicate that the potential barrier heights and trap minimum almost linearly increase by increasing the magnetization.

Another single permanent magnetic microtrap consisting of three rectangular permanent magnetic slabs with two different thicknesses of t_1 and t_2 and separation of d in a slightly different arrangement with respect to the U-shaped configuration is also investigated. Schematic of this structure is shown in figure 3. According to figure 4, by changing a bias field $\mathbf{B}_1 = B_{1z}\hat{z}$, it is possible to vary the barrier heights in the H-like-shaped atom chip.

This configuration of permanent magnetic slabs differs from the previous one in terms of fabrication and also possibility of movement of the magnetic slabs which allows for mechanically varying (coarse adjustment) the trap depth and frequencies. Numerical results given in figure 4 show that, this H-like-shaped microstructure can produce a minimum of magnetic potential in the space between parallel slabs above the middle one. These slabs can be set up on a table with any possible and desired separations and again a 3D Ioffe-Pritchard magnetic microtrap can be created even without a bias magnetic field. If we change B_{1z} , the trap frequencies change. Table 3 shows these values for the H-like-shaped atom chip with both values of low magnetization $4\pi M \sim 800$ G and high magnetization $4\pi M \sim 3800$ G on different scales. As plots in figures 4(d), 4(e) and 4(f) show, change of the external field does not change location of the microtrap center.

Table 2. More details about U-shaped microtraps. Values have been obtained numerically for ^{87}Rb in $F=2$ and $m_F=2$ state.

Parameter	Definition	Scale A_U		Scale A_U	
		0	1	0	3
$B_{1z}(\text{G})$	z component of bias field				
$4\pi M(\text{G})$	Magnetization of slabs	800		3800	
$\Delta U^x/k_B$ (mK)	Potential barrier height in x -direction	0.22	0.17	1	0.87
$\Delta U^y/k_B$ (mK)	Potential barrier height in y -direction		19		87
$\Delta U^z/k_B$ (mK)	Potential barrier height in z -direction		0.13		0.67
$\hbar\omega_x/k_B$ (μK)	Energy level spacing in x -direction	2.0	1.5	0.42	0.35
$\hbar\omega_y/k_B$ (μK)	Energy level spacing in y -direction	2.0	1.5	0.42	0.35
$\hbar\omega_z/k_B$ (μK)	Energy level spacing in z -direction		0.5		1.0

Curvatures of the magnetic field close to the center of the microtrap also change by variation of the bias field, as table 3 shows. Curves in figure 4 have been plotted for this configuration on scale A_H with $h = 80\mu\text{m}$, $a_1 = 2\mu\text{m}$, $a_2 = 3\mu\text{m}$, $d = 16\mu\text{m}$, $t_1 = 200\text{nm}$ and $t_2 = 250\text{nm}$, where $4\pi M \sim 800\text{G}$. Initial and final values of the potential barrier heights $\Delta U^i/k_B$ and energy level spacings $\omega_i/2\pi$ are also presented in table 4. Our investigations show that, movement of the parallel slabs in the H-like-

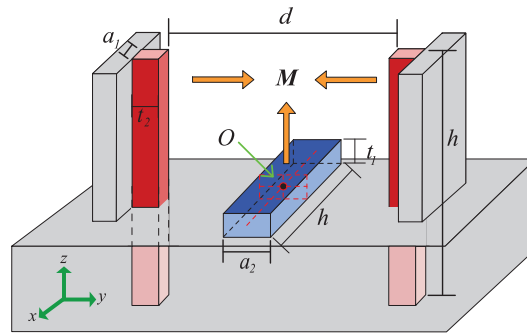


Figure 3. (color online). Schematic of an H-like-shaped permanent magnetic microtrap. The middle (blue) slab has a thickness of t_1 and thickness of the parallel (red) ones is t_2 . Also, separation between the parallel slabs is d . Magnetization is perpendicular to slabs (Orange arrows). All three slabs have same length h . Width of the parallel slabs is a_1 while that of the other slab is a_2 .

shaped microstructure can also change the depth of the microtrap. It is possible to

mechanically reduce the depth of the microtrap via increasing the separation between the parallel slabs. However it should be done adiabatically to avoid heating of atomic cloud. Previously, various methods have been used to load Bose-Einstein condensates and Fermi gases into microtraps; loading clouds of atoms at constant phase space density by magnetic transfer is one of the adiabatic transfer methods [19]. U- and H-like-shaped traps may also be useful for the displacement of clouds of atoms. There are lots of useful methods for the creation of these structures, like: Physical Vapour Deposition, Pulsed Laser Deposition and also Additive Patterning Lithography.

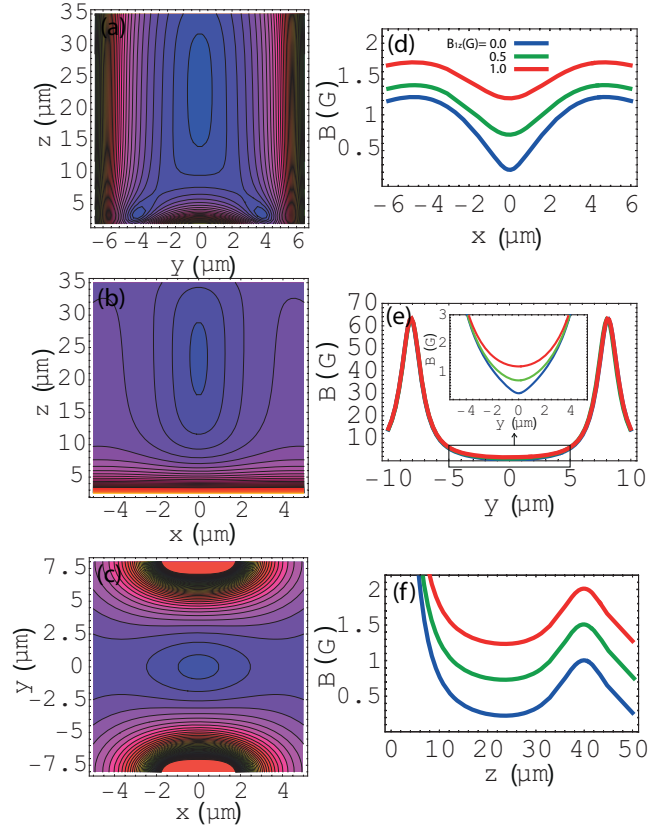


Figure 4. (Color online) (a), (b), (c) Contour plots of magnetic fields in $x = x_{min}$, $y = y_{min}$ and $z = z_{min}$ planes, respectively when external bias field is zero. Center of the microtrap is at $x_{min} = y_{min} = 0$ and $z_{min} = 23.6 \mu\text{m}$ above the middle slab. (d), (e) and (f) Plots of magnetic field along x , y and z directions, respectively, for $B_{1z} = 0, 0.5$ and 1.0 G. By increase of the bias magnetic field, the potential barrier heights in the x and y directions are reduced. Moreover, the bias field does not change the position of the microtrap center. Furthermore, B_{min} is 0.23 G when the bias field is zero. This figure describes the magnetic field modulus for the H-like-shaped atom chip shown in figure 3 for relatively small configuration $h=80\mu\text{m}$, $a_1=2\mu\text{m}$, $a_2=3\mu\text{m}$, $d=16\mu\text{m}$, $t_1 = 200\text{nm}$ and $t_2 = 250\text{nm}$, where $4\pi M \sim 800$ G.

3. Holding ultracold atoms and Bose-Einstein condensates

A BEC transition temperature of $T_c = 1.6 \mu\text{K}$ at a trap depth of $11 \mu\text{K}$ via RF evaporative cooling has been reported for ^{87}Rb atoms in an F-shaped fully permanent magnetic atom chip [27]. Without considering the interactions between atoms, for a 3D anisotropic harmonic oscillator, T_c is given by [3]

$$T_c \approx 4.5 \left(\frac{\bar{f}}{100 \text{Hz}} \right) N^{1/3} n K, \quad (1)$$

where \bar{f} and N are the geometric mean of the three trap frequencies $f_i = \omega_i/2\pi$, and number of atoms, respectively. In the presence of interactions, we should include the correction

$$\frac{\delta T_c}{T_c} \approx -0.73 \frac{\omega_m}{\bar{\omega}} N^{-1/3} - 1.33 \frac{a}{\bar{a}} N^{1/6}, \quad (2)$$

where \bar{a} , ω_m and a_s are $\sqrt{\hbar/2\pi m \bar{f}}$, $(\omega_x + \omega_y + \omega_z)/3$ and s-wave scattering length, respectively [54]. Since $\delta T_c/T_c$ has a negative value, the corrected transition temperature is less than the temperature given by equation (1). In the absence of any bias field, taking into account the interactions between atoms, BEC critical temperature for 10^6 ^{87}Rb atoms in different configurations U- and H-like-shaped microtraps, are predicted in the ranges $6.9\text{-}11\mu\text{K}$ and $12\text{-}16\mu\text{K}$, respectively. These relatively high BEC transition temperatures for 10^6 ^{87}Rb atoms are obtained due to high curvatures in center of the microtraps, which is essential property of permanent magnetic microtraps. However, these temperatures compared with experimentally achieved value of $1.6\mu\text{K}$ are not improbable. If high magnetization is used for microtraps, then height of the magnetic potential energy lets us to confine thermal atoms. For example, U-shaped trap with high magnetization of $4\pi M = 3800\text{G}$ can trap cold atoms with mean temperature of approximately $150 \mu\text{K}$. This temperature is roughly doppler cooling limit of Rb atoms in MOT. Therefore It is possible to directly load the atomic cloud from MOT to this trap and hold them without any bias field. With RF field and increasing external magnetic field, we can perform evaporative cooling. When the bias field is slowly increased, the barrier height in the x direction is lowered and atoms in the higher energy levels leave the trap. In the U and H-like-shaped traps, increasing the external magnetic field can reduce the trap depth and decrease the average temperature of atoms down to around $10 \mu\text{K}$ and below where numerical calculations predict that we attain BEC. During evaporative cooling, trap requires non-zero minimum for preventing spin flip loss. After achieving the BEC, the bias field must be slowly removed in order to increase the trap barrier heights for holding the Bose-Einstein condensate.

In high density ranges under $p \approx 10^{-11}$ Torr, two-body spin relaxation and three-body recombination are two dominant loss mechanisms. The corresponding loss rate is obtained by [3].

$$\Upsilon = \frac{1}{n} \frac{dn}{dt} \approx nG + Ln^2, \quad (3)$$

Table 3. Numerical results for H-like-shaped fully permanent magnetic atom chip shown in figure 1. Results are obtained for ^{87}Rb in $F=2$ and $m_F=2$ state with two values of magnetization $4\pi M \sim 800$ G and $4\pi M \sim 3800$ G. On scale A_H , we have $h=80\mu\text{m}$, $a_1=2\mu\text{m}$, $a_2=3\mu\text{m}$, $d=16\mu\text{m}$, $t_1 = 200\text{nm}$ and $t_2 = 250\text{nm}$. Scale B_H is two times larger than scale A_H .

Parameter	Scale A_H		Scale A_H		Scale B_H	
	0	1	0	3	0	3
$B_{1z}(\text{G})$						
$4\pi M(\text{G})$	800		3800		3800	
$\frac{\partial^2 B}{\partial x^2} (\frac{\text{G}}{\text{cm}^2})$	8.9×10^5	1.6×10^5	4.2×10^6	1.14×10^6	1.07×10^6	2.8×10^5
$\frac{\partial^2 B}{\partial y^2} (\frac{\text{G}}{\text{cm}^2})$	8.9×10^5	1.6×10^5	4.2×10^6	1.14×10^6	1.07×10^6	2.8×10^5
$\frac{\partial^2 B}{\partial z^2} (\frac{\text{G}}{\text{cm}^2})$	3.8×10^3		4.4×10^3		3.8×10^3	
$\omega_x/2\pi(\text{kHz})$	12	5.2	26.3	13.6	13	6.8
$\omega_y/2\pi(\text{kHz})$	12	5.2	26.3	13.6	13	6.8
$\omega_z/2\pi(\text{kHz})$	0.78		1.71		0.8	
$z_{min} (\mu\text{m})$	23.6		23.6		47.17	
$B_{min} (\text{G})$	0.23	1.23	1.1	4.1	1.1	4.1

where n , G and L are density, the two-body spin-relaxation and three-body-recombination coefficients, respectively. For density of alkali atoms around $n=10^{12}-10^{14}$ atoms/cm³, loss rate is usually about $10^{-3}-10^{-1}$ s⁻¹. As an example, on scale A for the U trap (A_U in table 1) with particle number $N=10^6$ for ^{87}Rb atoms, density is 3×10^{13} atoms/cm³ and we have $\Upsilon \sim 0.05\text{s}^{-1}$, while for the scale C_U , density reduces to 6.4×10^{12} atoms/cm³ and relatively low loss rate of $\Upsilon \sim 7 \times 10^{-3}\text{s}^{-1}$ is obtained which allows for achieving a BEC with high atom numbers. Here, $G < 10^{-15}\text{cm}^3/\text{s}$ [55] and $L=1.8 \times 10^{-29}\text{cm}^6/\text{s}$ [49].

4. Conclusions

To summarize, we have introduced two fully permanent magnetic atom chips to confine, hold and manipulate ultracold atoms. We have suggested using external magnetic fields together with RF waves to reduce potential barrier heights of the permanent magnetic microtraps for more efficient evaporative cooling. Considering the high magnetic field curvatures in permanent microtraps compared with those of current-carrying wires and optical traps, the BEC critical temperature T_C is predicated to locate in the μK ranges however loss mechanisms are strong. Potential barrier heights of the microtraps linearly depend on the magnetization of slabs. For cooling and trapping thermal clouds of atoms, highly magnetized materials must be used in microtrap structures to increase the minimum of trap, potential height and trap frequencies. If smaller magnetic curvatures and trap frequencies are required in certain potentials heights, then large scale configurations can be useful. These large scale atom chips provide relatively large

Table 4. More details about H-like-shaped microtraps. Values have been obtained numerically for ^{87}Rb in $F=2$ and $m_F=2$ state.

Parameter	Definition	Scale A_H		Scale A_H	
		0	1	0	3
$B_{1z}(\text{G})$	z component of bias field				
$4\pi M$ (G)	Magnetization of slabs	800		3800	
$\Delta U^x/k_B$ (μK)	Potential barrier height in x -direction	70	34	250	140
$\Delta U^y/k_B$ (mK)	Potential barrier height in y -direction	4.2		20.15	
$\Delta U^z/k_B$ (μK)	Potential barrier height in z -direction	55		260	
$\hbar\omega_x/k_B$ (μK)	Energy level spacing in x -direction	0.58	0.25	1.26	0.65
$\hbar\omega_y/k_B$ (μK)	Energy level spacing in y -direction	0.58	0.25	1.26	0.65
$\hbar\omega_z/k_B$ (μK)	Energy level spacing in z -direction	0.03		0.08	

volumes for achieving the BEC with high atom numbers and low atom loss. Due to their very high confinement, these microtraps may be suitable for single atom experiments for quantum information processing. Another advantage of these microtraps is that they can store ultracold atoms and Bose-Einstein condensates without any external bias field. These permanent magnetic atom chips may be used together with other atom chips as promising tools for the investigation of quantum degenerate gases. Such applications of these new types of microtraps should have a good impact on the development of the atom chip field. The fully permanent magnetic micro-structures presented here are very simple and the dimensions and magnetization of the magnetic slabs are within the accessible ranges of the contemporary technology. Depending on the magnetization of slabs, cold atoms can be loaded directly or after intermediate cooling stages from the MOT to these microtraps.

Acknowledgments

The authors would like to thank Peter Hannaford, Bryan Dalton and Brenton Hall for helpful discussions and comments.

References

- [1] Anderson M H, Ensher J R, Matthews M R, Wieman C E and Cornell E A 1995 Observation of Bose-Einstein Condensation in a Dilute Atomic Vapor *Science* **269** 198.

- [2] Davis K B, Mewes M -O, Andrews M R, van Druten N J, Durfee D S, Kurn D M and Ketterle W 1995 Bose-Einstein Condensation in a Gas of Sodium Atoms *Phys. Rev. Lett.* **75** 3969.
- [3] Pethick C J and Smith H 2008 Bose-Einstein condensation in dilute gases, 2nd Ed Cambridge University Press.
- [4] Leggett A 2001 Bose-Einstein condensation in the alkali gases: Some fundamental concepts *Rev. Mod. Phys.* **73** 307.
- [5] Metcalf H J and Straten P 2002 Laser Cooling and Trapping, Springer.
- [6] Barrett M D, Sauer J A and Chapman M S 2001 All-Optical Formation of an Atomic Bose-Einstein Condensate *Phys. Rev. Lett.* **87** 010404.
- [7] Sun K, Liu W V, Hemmerich A and Sarma S D 2012 Topological semimetal in a fermionic optical lattice *Nat. Phys.* **8** 67.
- [8] Hinds E A, Boshier M G and Hughes I G 1998 Magnetic waveguide for trapping cold atom Gases in Two Dimensions *Phys. Rev. Lett.* **80** 645.
- [9] Dekker N H, Lee C S, Lorent V, Thywissen J H, Smith S P, Drndi M, Westervelt R M and Prentiss M 2000 Guiding Neutral Atoms on a Chip *Phys. Rev. Lett.* **84** 1124.
- [10] Nguyen S V, Helton J S, Maussang K, Ketterle W and Doyle J M 2005 Magnetic trapping of an atomic ^{55}Mn - ^{52}Cr mixture *Phys. Rev. A* **71** 025602.
- [11] Weinstein J D and Libbrecht K G 1995 Microscopic magnetic traps for neutral atoms *Phys. Rev. A* **52** 4004.
- [12] Esslinger T, Bloch I and Hänsch T W 1998 Bose-Einstein condensation in a quadrupole-Ioffe-configuration trap *Phys. Rev. A* **58** R2664.
- [13] Fortagh J, Grossman A, Zimmermann C and Hänsch T W 1998 Miniaturized Wire Trap for Neutral Atoms *Phys. Rev. Lett* **81** 5310.
- [14] Yin J, Gao W, Hu J and Wang Y 2002 Magnetic surface microtraps for realizing an array of alkali atomic Bose-Einstein condensates or Bose clusters *Opt. Commun.* **206**, 99.
- [15] Müller D, Anderson D Z, Grow R J, Schwindt P D D and Cornell E A 1999 Guiding Neutral Atoms Around Curves with Lithographically Patterned Current-Carrying Wires *Phys. Rev. Lett.* **83** 5194.
- [16] Grabowski A and Pfau T 2003 A lattice of magneto-optical and magnetic traps for cold atoms *Eur. Phys. J. D* **22** 347.
- [17] Reichel J Hänsel W and Hänsch T W 1999 Atomic micromanipulation with magnetic surface traps *Phys. Rev. Lett.* **83** 3398.
- [18] Du S, Squires M B, Imai Y, Czaia L, Saravanan R A, Bright V, Reichel J, Hnsch T W and Anderson D Z 2004 Atom-chip Bose-Einstein condensation in a portable vacuum cell *Phys. Rev. A* **70** 053606.
- [19] Fortágh J and Zimmermann C 2007 Magnetic microtraps for ultracold atoms *Rev. Mod. Phys.* **79** 235.
- [20] Ricci L Zimmermann C Vuletic V and Hansch T W 1994 Generation of cylindrically symmetrical magnetic-fields with permanent-magnets and mu-metal *Appl. Phys. B* **59** 195.
- [21] Hinds E A and Hughes I G 1999 Magnetic atom optics: mirrors, guides, traps, and chips for atoms *J. Phys. D: Appl. Phys.* **32** R119.
- [22] Ghanbari S kieu T D, Sidorov A and Hannaford P 2006 Permanent magnetic lattices for ultracold atoms and quantum degenerate gases *J. Phys. B* **39** 847.
- [23] Boyd M, Streed E W, Medley P, Campbell G K, Mun J, Ketterle W and Pritchard D E 2007 Atom trapping with a thin magnetic film *Phys. Rev. A* **76** 043624.
- [24] Gerritsma R, Whitlock S, Fernholz T, Schlatter H, Luigjes J A, Thiele J -U, Goedkoop J B and Spreeuw R J C 2007 Lattice of microtraps for ultracold atoms based on patterned magnetic films *Phys. Rev. A* **76** 033408.
- [25] Ghanbari S, kieu T D and Hannaford P 2007 A class of permanent magnetic lattices for ultracold atoms *J. Phys. B: At. Mol. Opt. Phys.* **40** 1283.
- [26] Mohammadi A, Ghanbari S and Pariz A 2013 A two-dimensional permanent magnetic lattice for

- ultracold atoms *Phys. Scr.* **88** 015601
- [27] Fernholz T, Gerritsma R, Whitlock S, Barb I and Spreeuw R J C 2008 Fully permanent magnet atom chip for Bose-Einstein condensation *Phys. Rev. A* **77** 033409.
- [28] Schmied R, Leibfried, D Spreeuw R J C and Whitlock S 2010 Optimized magnetic lattices for ultracold atomic ensembles *New J. Phys.* **12** 103029.
- [29] Garca I L, Darquie B, Curtis E A, Sinclair C D J and Hinds E A 2010 Experiments on a videotape atom chip: fragmentation and transport studies *New J. Phys.* **12** 093017.
- [30] Weber M T, Herbig J, Mark M, Nagerl H -C and R Grimm R 2003 Bose-Einstein condensation of cesium *Science* **299** 232.
- [31] Cornell E 1996 Very cold indeed: the nanokelvin physics of Bose-Einstein condensation *J. Res. Natl. Inst. Stand. Technol.* **101** 419.
- [32] Hall B V, Whitlock S, Scharnberg F, Hannaford P and Sidorov A 2006 A permanent magnetic film atom chip for Bose-Einstein condensation *J. Phys. B* **39** 27.
- [33] Vuletic V, Fischer T, Praeger M, Hansch T W and Zimmermann C 1998 Microscopic Magnetic Quadrupole Trap for Neutral Atoms with Extreme Adiabatic Compression *Phys. Rev. Lett.* **80** 1634.
- [34] Bradley C C, Sackett C A and Hulet R G 1997 Bose-Einstein Condensation of Lithium: Observation of Limited Condensate Number *Phys. Rev. Lett.* **78** 985.
- [35] Du S and Oh E 2009 Three-wire magnetic trap for direct forced evaporative cooling *Phys. Rev. A* **79** 013407).
- [36] Folman R, Kruger P, Schmiedmayer J, Denschlag J and Henkel C 2002 Microscopic atom optics: From wires to an atom chip *Adv. At. Mol. Opt. Phys.* **48** 263.
- [37] Ott H, Fortagh J, Schlotterbeck G, Grossmann A and Zimmermann C 2001 Bose-Einstein condensate in a surface microtrap *Phys. Rev. Lett.* **87** 230401.
- [38] Cano D, Kasch B, Hattermann H, Kleiner R, Zimmermann C, Koelle D and Fortagh J 2008 Meissner Effect in Superconducting Microtraps *Phys. Rev. Lett.* **101** 183006.
- [39] Greiner M, Mandel O, Esslinger T, Hansch T W and Bloch I 2002 Quantum phase transition from a superfluid to a Mott insulator in a gas of ultracold atoms *Nature* **415** 39.
- [40] Wang Y J, Anderson D Z, Bright V M, Cornell E A, Diot Q, Kishimoto T, Prentiss M, Saravanan R A, Segal S R and Wu S 2005 Atom Michelson Interferometer on a Chip Using a Bose-Einstein Condensate *Phys. Rev. Lett.* **94** 090405.
- [41] Jo G -B, Choi J-H, Christensen C A, Lee Y -R, Pasquini T A, Ketterle W and Pritchard D E 2007 Matter-Wave Interferometry with Phase Fluctuating Bose-Einstein Condensates *Phys. Rev. Lett.* **99** 240406.
- [42] Schumm T, Hofferberth S, Andersson L M, Wildermuth S, Groth S, Bar-Joseph I, Schmiedmayer J and Kruger P 2005 Matter-wave interferometry in a double well on an atom chip *Nat. Phys.* **1** 57.
- [43] Ghanbari S, Blakie P B, Hannaford P and Kieu T D 2009 Superfluid to Mott insulator quantum phase transition in a 2D permanent magnetic lattice *Eur. Phys. J. B* **70** 305.
- [44] Guglielmino M, Penna V and Capogrosso-Sansone B, 2010 Mott-insulator to superfluid transition in Bose-Bose mixtures in a two-dimensional lattice *Phys. Rev. A* **82** 021601(R).
- [45] Cirone M A, Negretti A, Calarco T, Kruger P and Schmiedmayer J 2005 A simple quantum gate with atom chips *Eur. Phys. J. D* **35** 165.
- [46] Birkel G and J Fortagh J 2007 Micro traps for quantum information processing and precision force sensing *Laser-Photon. Rev* **1** 12.
- [47] Tejada J, Chudnovsky E M, del Barco E, Hernandez J M and Spiller T P 2001 Magnetic qubits as hardware for quantum computers *Nanotechnology* **12** 181.
- [48] Riedel M F, Bohi P, Li Y, Hansch T W, Sinatra A and Treutlein P 2010 Atom-chip-based generation of entanglement for quantum metrology *Nature* **464** 1170.
- [49] Soding J, Guery-Odelin D, Desbiolles P, Chevy F, Inamori H and Dalibard J 1999 Three-body decay of a rubidium Bose-Einstein condensate *Applied Physics B* **69** 257.

- [50] Stuart B G, Clauser H R and Vaccari J A, 2002 *Materials Handbook: An Encyclopedia for Managers McGraw-Hill Professional*, 577.
- [51] Mantovan R, Georgieva M, Perego M, Lu H L, Cocco S, Zenkevich A, Scarel G and Fanciulli M 2007 Atomic Layer Deposition of Magnetic Thin Films *ACTA PHYSICA POLONICA A* **112** N.6.
- [52] Edited by Nalwa H S 2002 *Handbook of Thin Film Materials* **1** Academic Press, New York.
- [53] Available from: <http://www.esrf.eu/Accelerators/Groups/InsertionDevices/Software/Radia>.
- [54] Giorgini S, Pitaevskii L P and Stringari S 1996 Condensate fraction and critical temperature of a trapped interacting Bose gas *Phys. Rev. A* **54** R4633.
- [55] Boesten H M J M, Moerdijk A J and Verhaar B J 1996 Dipolar decay in two recent Bose-Einstein condensation experiments *Phys. Rev. A* **54** R29.